

Journal of Experimental and Applied Physics

Journal Homepage: jeap.ppj.unp.ac.id Vol. 3, No. 3, September 2025.

SSN (Print): 2988-0378 ISSN (Online): 2987-9256



Seismicity Level Analysis of the West Coast of Northern Sumatra in 1964-2023 based on Spatial and Temporal Variations of Seismotectonic Parameters

Moreno Wahyu Arieza^{1,*}, Puji Ariyanto¹

¹Department of Geophysics, State College of Meteorology, Climatology, and Geophysics (STMKG), Tangerang 15119, Indonesia

Article History

Received: May, 05th 2025 Revised: June, 22nd 2025 Accepted: July, 18th 2025 Published: September, 30th 2025

DOI:

https://doi.org/10.24036/jeap.v3i3.102

Corresponding Author

*Author Name: Moreno Wahyu Arieza

Email: ariezamorenoo@gmail.com

Abstract: Located in the subduction zone of the Indo-Australian Plate beneath the Eurasian Plate, the west coast of northern Sumatra experiences high seismic activity, as evidenced by the 2004 Aceh earthquake (Mw9.1) and the 2005 Nias-Simeulue earthquake (Mw8.6). This study analyzes the spatial and temporal variations of b-values and a-values to evaluate rock stress accumulation and seismicity levels as a basis for earthquake hazard mitigation. The analysis uses the Maximum Likelihood method based on the Gutenberg-Richter law. Earthquake data were obtained from the USGS catalog (1964–2023), filtered for events of Mw ≥ 5.0 and focal depths < 60 km within 2.01°S-7.54°N and 92.77°E-99.45°E. Compared to previous studies, this work provides extended temporal coverage and finer spatial resolution, enabling a more comprehensive assessment of spatial and temporal variations in seismotectonic parameters. The inclusion of recurrence interval analysis for Mw ≥ 7.0, 8.0, and 9.0 enhances understanding of regional seismic hazards. Results show that b-values range from 0.53-2.07 and a-values from 4.3-12.45. Nagan Raya and Aceh Singkil exhibit both low b- and a-values, indicating high stress accumulation and low seismicity-conditions linked to higher earthquake potential. Estimated return periods in these areas are 17.6–210.3 years (Nagan Raya) and 15.7–208.8 years (Aceh Singkil) for increasing magnitudes. These estimates carry uncertainty due to data and model limitations but remain crucial for preparedness planning. Identifying zones with high stress and short recurrence periods provides practical input for prioritizing mitigation efforts and reducing earthquake risk in northern Sumatra.

Keywords: *a*-value; *b*-value; northern Sumatra; seismic hazard; seismotectonic parameters.



Journal of Experimental and Applied Physics is an open access article licensed under a Creative Commons Attribution ShareAlike 4.0 International License which permits unrestricted use, distribution, and reproduction in any medium, provided the original work is properly cited. ©2024 by author.

How to cite:

1. Introduction

Sumatra Island is well known for its complex tectonic configuration, attracting the attention of many researchers in the fields of geology and earth sciences. This complexity arises from two major tectonic systems with significant implications for regional seismicity. The first is the subduction zone where the Indo-Australian Plate subducts beneath the Eurasian Plate [1]. The second is the Sumatran Fault Zone (SFZ), also known as the Semangko Fault, a major strike-slip fault system extending along the island [2].

The western part of Sumatra, located in Indonesia, is particularly prone to seismic activity due to both the Great Sumatran Fault—comprising segments such as Sumpar, Sianok, and Sidak—and the offshore subduction zone along its west coast. This subduction zone is considered the youngest in Indonesia and is characterized by a shallow dip angle, which results in strong interplate coupling and an increased potential for large-magnitude earthquakes.

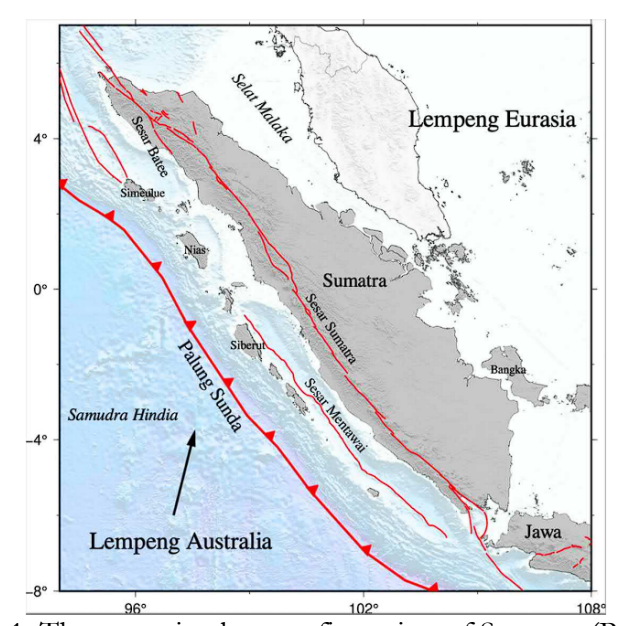


Figure 1. The tectonic plate configuration of Sumatra (Pusgen 2022)

Historical earthquake records show that several large-magnitude events have occurred in the northern part of western Sumatra, including the 2004 Aceh earthquake (Mn9.1), which generated a devastating tsunami, and the 2005 Nias earthquake (Mn8.6). These events highlight the urgent need for a fundamental seismicity study in this region. Such studies utilize parameters like b-value, a-value, and Mc (magnitude of completeness) to assess seismic behavior. The b-value reflects the level of stress accumulation within the crust, where a higher b-value generally indicates more fractured rocks and lower stress concentration [3]. The a-value, on the other hand, represents the overall seismicity level, with higher values corresponding to more frequent earthquakes [4]. Meanwhile, Mc denotes the minimum magnitude at which an earthquake can be reliably detected by the seismic network, ensuring data completeness [5].

In this research, the cumulative frequency–magnitude distribution is utilized to estimate Mc, which is essential for determining reliable *b*- and *a*-values. These seismotectonic parameters are widely used in seismicity and seismic hazard assessments [4,6].

The primary objective of this study is to characterize the seismic behavior of the northern west coast of Sumatra by analyzing spatial and temporal variations in *b*-value, *a*-value, and *Mc*. This approach also seeks to interpret the physical significance of *b*-value variation and its correlation

with stress accumulation and seismic hazard potential in the study area. The novelty of this research lies in the use of a longer temporal dataset (1964–2023) and finer spatial resolution grids, which enable a more detailed and statistically robust assessment of seismotectonic behavior. Building upon previous studies that examined seismicity in the region, this research expands the temporal scope and improves spatial resolution by using earthquake data from 1964 to 2023 and a finer analysis grid. It also incorporates recurrence interval analysis for multiple magnitude thresholds ($Mw \ge 7.0$, 8.0, and 9.0), offering practical insights into earthquake potential at the district level. These advancements support a more refined identification of high-risk zones, thereby contributing to improved regional seismic hazard assessments and more focused mitigation planning.

2. Materials and Method

This research employs earthquake data from the west coast of the northern Sumatra region spanning from 1964 to 2023. The earthquake data was acquired from the USGS (United States Geological Survey) catalog within the coordinates of 2.01°S – 7.54°N latitude and 92.77°E – 99.45°E longitude covering the period from January 1, 1964, to July 30, 2023. The data includes earthquake locations (latitude and longitude), magnitudes, origin times, and depths.

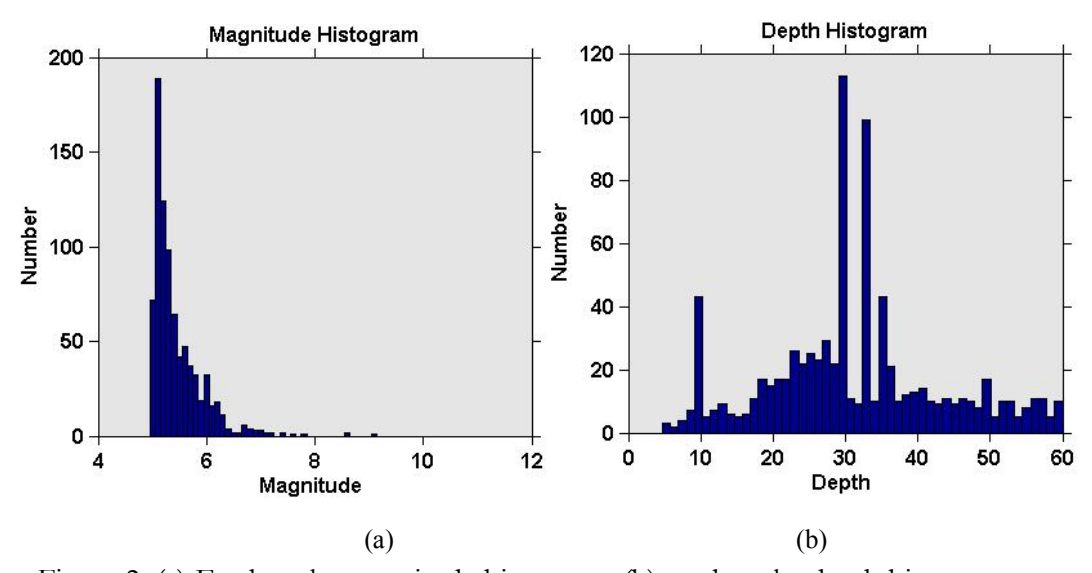


Figure 2. (a) Earthquake magnitude histogram, (b) earthquake depth histogram.

The earthquake parameters are limited to significant and shallow earthquakes with a moment magnitude (*Mw*) range of 5.0 and depths from 0.9 km to 60 km. The frequency distribution of earthquake magnitudes shows the highest frequency at magnitude *Mw*5.1, while the frequency distribution of earthquake depths shows the highest frequency at depths of 30 km and 10 km due to fixed depth values for some earthquakes in the USGS catalog, as shown in Figure 2(a) and Figure 2(b).

The spatial distribution of clustered earthquake data is presented based on depth using the Generic Mapping Tools (GMT) program. Earthquakes with depths less than 15 km are represented by red circles, those between 15-30 km by yellow circles, and those with depths between 30-60 km are depicted with green circles. Star symbols represent earthquakes with a magnitude of *Mw9.1*, and the most powerful earthquakes recorded during the research period, as shown in Figure 3.

The total earthquake data initially amounted to 1101 earthquakes but decreased to 836 (a reduction of 24.07%) after declustering. Declustering involved removing foreshocks and aftershocks to obtain the mainshock earthquake data, which better represents earthquake characteristics with higher accuracy [6].

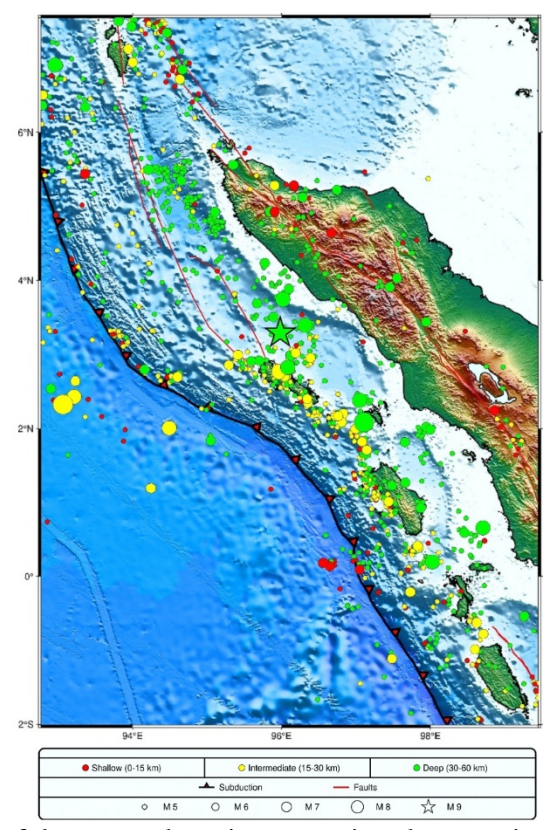


Figure 3. Seismicity map of the research region, covering the magnitude range of Mw5.0 to Mw9.1 and depths ranging from 0.9 to 60 km, was generated using USGS catalog data from the period 1964 to 2023. This map was created with GMT (Generic Mapping Tools)

The calculation of values a and b is based on the Gutenberg-Richter equation, where the relationship between earthquake frequency distribution and magnitude is given by:

$$\log_{10} N(M) = a - bM$$

Where N(M) represents the number of earthquakes with a magnitude greater than or equal to the target value M, and the values b and a are positive constants representing the seismicity level and the slope of the cumulative earthquake magnitude-frequency curve, respectively [7]. The value of b in this study is calculated using the Aki equation [8], expressed as follows: $b = \frac{\log_{10} e}{\left(M_{\text{avg}} - M_{\text{min}}\right)}$

$$b = \frac{\log_{10} e}{\left(M_{\text{avg}} - M_{\text{min}}\right)}$$

Where M_{avg} represents the average magnitude of all earthquakes with $M \geq M_c$.

The ZMAP6.0 program [9] is used to calculate the spatio-temporal variations of values a and b using the Maximum-Likelihood method, as well as the magnitude of completeness M_c and the earthquake recurrence interval for $M_w \ge 7.0$, $M_w \ge 8.0$, and $M_w \ge 9.0$. The Maximum

Likelihood method has been used in previous studies for calculating b-values, a-values, and estimating M_c using the Gutenberg-Richter law as a function of the lowest magnitude [10].

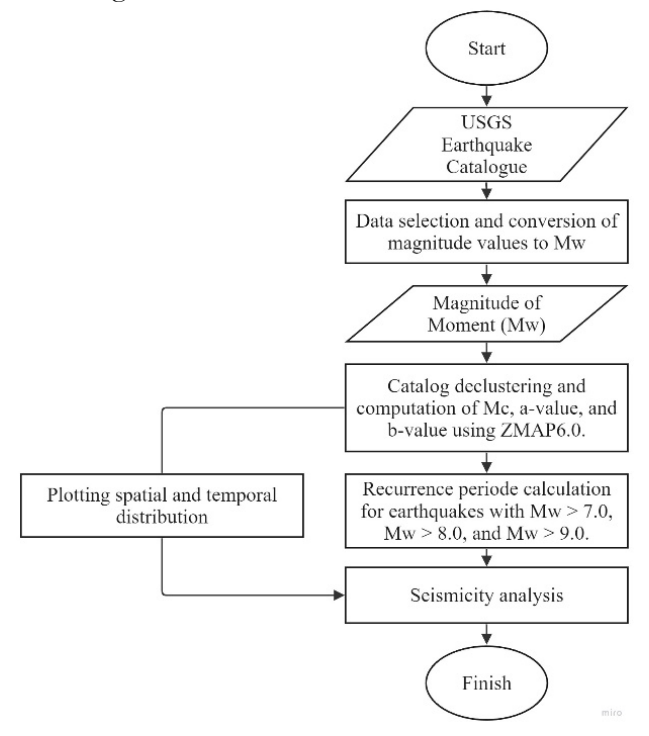


Figure 4. Data processing flowchart.

Through the ZMAP6.0 program, the study area is divided into a grid of $0.1^{\circ} \times 0.1^{\circ}$, a resolution commonly adopted in previous seismotectonic studies to capture spatial heterogeneity without sacrificing statistical reliability [11], [12], [13]. This grid size offers a practical balance: it is fine enough to resolve local variations in *b*-values and *a*-values, yet broad enough to ensure that each cell contains a sufficient number of events for stable estimation. A minimum threshold of $N_{\min} \ge 10$ earthquakes, where $M \ge M_c$, is applied in each grid cell. While some studies use higher thresholds (e.g., 30–60 events) for greater statistical confidence [14], a threshold of 10 is often used in low to moderate seismicity regions to avoid excessive data loss, and is also supported as a minimum operational value in ZMAP's documentation. In general, the data processing steps follow the flowchart shown in Figure 4.

3. Results and Discussion

The subsequent calculation results provide spatial and temporal variation maps and earthquake recurrence intervals through mapping seismo-tectonic parameters. Figure 5. provides a map of the cumulative frequency distribution of magnitudes, which estimates the magnitude of completeness Mc [15]. The Mc value is necessary to obtain variations in the b-value and a-value in the research region. The results obtained through the Maximum Likelihood method yield a b-value of 0.912 with a standard error of 0.04, which closely approaches the 'normal value' $b \approx 1.0$, following the study conducted by Gui et al. [15]. However, it is important to note that the estimation of Mc and b-values may still be influenced by potential biases due to catalog incompleteness or limitations in detecting smaller-magnitude events, particularly in offshore or sparsely instrumented areas. These factors can lead to underrepresentation of low-magnitude earthquakes, thereby affecting the accuracy of frequency-magnitude distributions and seismotectonic parameter estimation.

Additionally, a value of a is determined to be 7.5, with an annual a-value of 5.73. The magnitude completeness Mc, which indicates the smallest magnitude that still fulfills the linearity of the Frequency-Magnitude Distribution (FMD) [10] from the USGS catalog, is found to be 5.2. The estimated values of b and a result in a linear-logarithmic relationship in the form of the Gutenberg-Richter equation, expressed as log10N = 7.5 - 0.912M, and is represented as the red linear line in Figure 5.

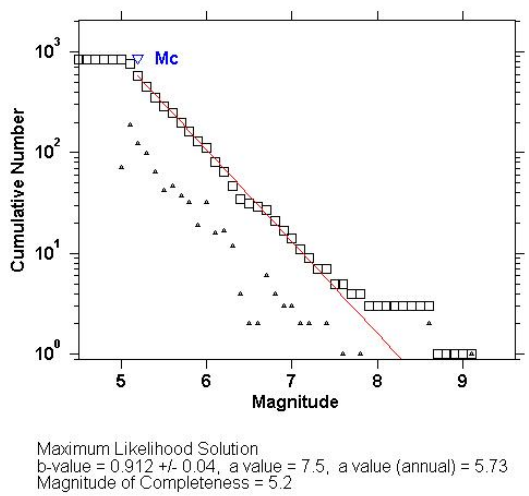


Figure 5. The Magnitude-Frequency distribution using the Maximum Likelihood method

The values of b and a generated are generally consistent with previous research results. The obtained b-value for the study area worldwide is around 1.02, with a standard error of 0.03 [16]. Meanwhile, in subduction zones, the b-value varies in the range of 0.70 to 1.50 [17], with the lowest b-values found in oceanic subduction zones, ranging from 0.53 to 0.72 for different tectonic conditions [18]. Pailopee et al. [18] conducted their research in a limited area of the northern segment of the Sumatra-Andaman subduction zone. They obtained b-value of 0.9, an annual a-value of 5.4, and Mc value of Mb5.0.

The *b*-value as a tectonic parameter at a seismic event location indicates the rock fragility level depending on the local rocks' natural conditions. The *b*-value is directly proportional to the degree of heterogeneity of the medium and inversely proportional to the level of rock stress [15]. With a *b*-value of 0.912, which is lower than the normal value, it indicates that the west coast of the northern Sumatra region has relatively high rock stress levels and low rock heterogeneity. Meanwhile, the *a*-value, as a seismicity parameter at 7.5 indicates a relatively high level of seismicity.

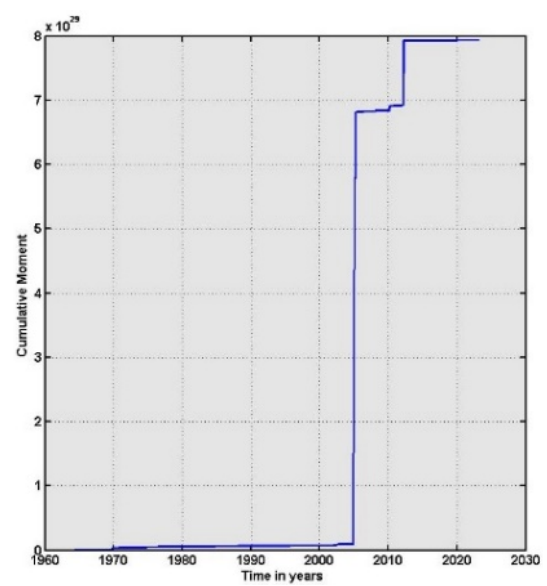


Figure 6. Cumulative moment release

Figure 6 illustrates the temporal pattern of moment release. Analyzing the cumulative moment release provides valuable insights into the total energy discharged by the fault system within a specific timeframe. Notably, we discern noteworthy spikes in seismic energy release preceding the earthquakes of 1979 (Mw7.9), 1996 (Mw8.1), 2002 (Mw7.6), and 2009 (Mw7.8). This observation is consistent with the research conducted by Jaume et al. [19]. Furthermore, Barajas et al. [20] concluded that the escalation in seismic moment release can be attributed to either an enlargement of the average fault size or the activation of pre-existing fault segments.

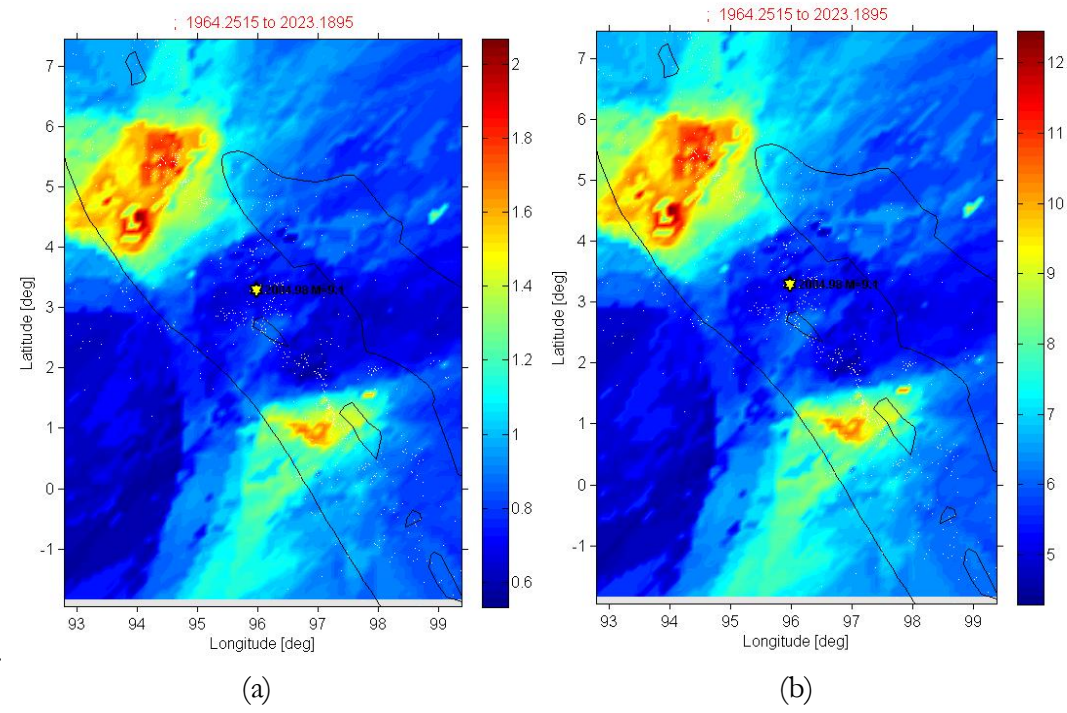


Figure 7. (a) Spatial variations plot of *b*-values, (b) spatial variations plot of *a*-values in research region.

The spatial variations plot of *b*-values (Figure 7(a)) results in a range of *b*-values from 0.53 to 2.07. The lowest *b*-values ranged (0.53-0.57), represented by dark blue, encompassing the Nagan Raya area and Aceh Singkil. The highest *b*-value (2.07), indicated by brown to reddish color, is observed in the Indian Ocean near the subduction zone to the northwest of Aceh regions surrounding the Batee Fault and the northern region of the Sumatra Fault Zone.

Research by Solorzano and Linkimer [21] concluded that *b*-values are generally higher in the upper-plate region than in the interplate region. The fault mechanism can also influence *b*-values, where areas dominated by strike-slip fault types in the upper-plate region tend to have higher *b*-values compared to regions with reverse fault types [18,19]. According to Serkan [24], *b*-values vary between 0.3 and 2.0, depending on the regional conditions of the study area. The results' differences are likely due to variations in the applied methods, including the seismic data clustering process, earthquake data completeness, and the uniformity of earthquake magnitude measurements [16].

The resulting variation in *a*-values falls within the range of 4.28 to 12.45. The lowest *a*-value (4.28-4.51) is observed in the Nagan Raya and Aceh Singkil areas, while the highest *a*-value (12.45) is observed in the Indian Ocean to the northwest of Aceh. The high *a*-value in the Indian Ocean to the northwest of the Aceh region aligns with the findings of a previous study by Arimuko [25], which concluded that the area around the northern west of the Mentawai Fault near the subduction zone experiences high seismicity.

The similarity between the *a-values* and *b*-values plots suggests that *b*-values influence the calculation of *a-values*. Low *b*-values indicate that rocks have accumulated high stress over a long period, which will be released as large earthquakes. Consequently, regions with low *b*-values typically have low seismicity levels, as low a-values indicate [26]. As for *b*-values, they are influenced by various factors. In addition to the frequency distribution of earthquake magnitudes, *b*-values are also affected by the level of rock stress in a region [27]. Medium heterogeneity, fault types, rock characteristics, and crustal structure also influence *b*-values in a region [28].

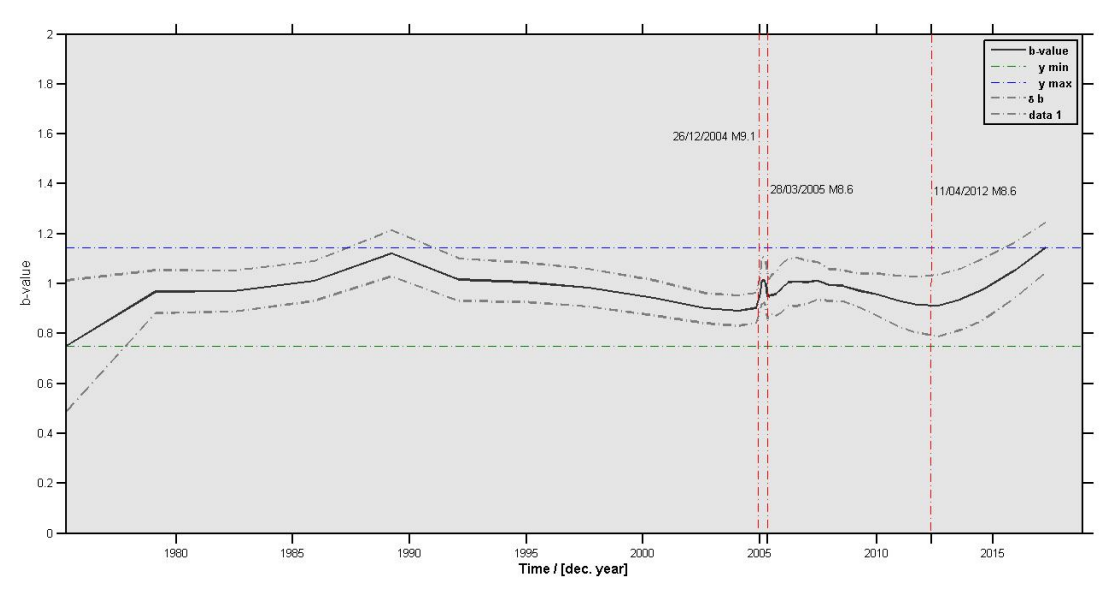


Figure 8. Temporal variations plot of *b*-values

Figure 8 illustrates the temporal variation plot of the *b*-value. The dashed blue horizontal lines indicate a maximum value of 1.14, while the dashed green horizontal lines represent a minimum value of 0.75. The dashed red vertical lines indicate significant earthquakes that occurred in the years 2004 (*Mn*9.1), 2005 (*Mn*8.6), and 2012 (*Mn*8.6). The figure also shows a decreasing trend in the *b*-values shortly before the significant earthquakes, consistent with the study conducted by Huang et al. [29]. This suggests a decrease in the *b*-values in certain regions, which could potentially

be used as a precursor to significant earthquakes. The decrease in the *b*-values may be attributed to increased rock stress levels [30].

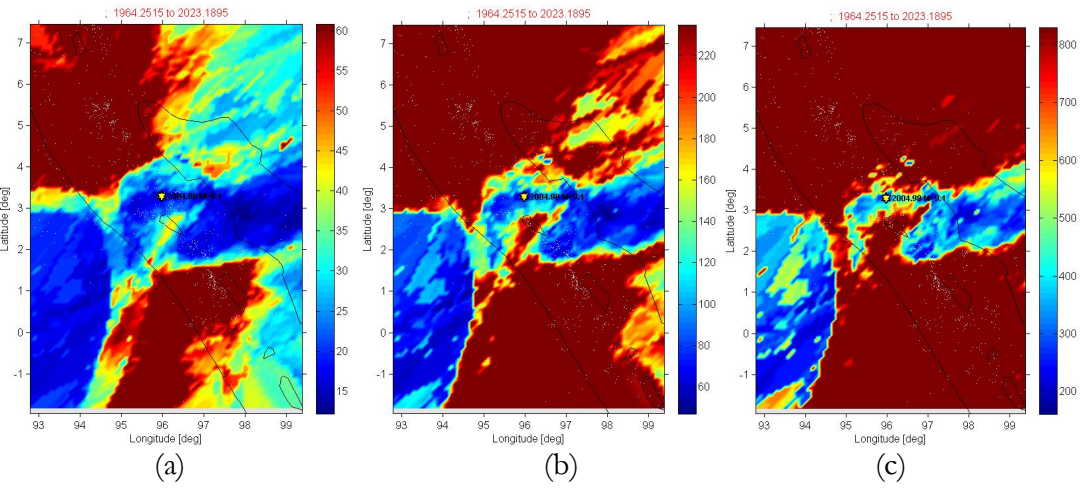


Figure 9. Recurrence period plot of (a) Mw>7.0, (b) Mw>8.0, (c) Mw> 9,0

Figure 9 illustrates the recurrence period plot for earthquakes with (a) Mw > 7.0, (b) Mw > 8.0, and (c) Mw > 9.0. The dark blue color indicates the lowest values, while the reddish-brown color indicates progressively higher values. Nagan Raya and Aceh Singkil regions have the lowest recurrence periods for $Mw \ge 7$, $Mw \ge 8$, and $Mw \ge 9$, respectively. For Nagan Raya, these periods are 17.6 years, 60.8 years, and 210.3 years, while for Aceh Singkil, they are 15.7 years, 57.3 years, and 208.8 years. Other areas with the lowest recurrence periods are Aceh Tenggara Regency, Subulussalam City, and Aceh Selatan Regency, with recurrence periods of 12-15 years for Mw > 7.0, 50-60 years for Mw > 8.0, and 160-200 years for Mw > 9.0. Generally, regions with low recurrence periods have low b-values. The recurrence periods for marked significant earthquakes are listed in Table 1.

Latitude (°)	Longitude (°)	Year -	Recurrence Period (Years)		
			Mw > 7.0	Mw > 8.0	Mw > 9.0
3.295	95.982	2004	35.3	247.4	1763.4
2.327	93.063	2005	15.9	63.5	256.2
2.085	97.108	2012	50.1	429.7	3732.2

Table 1. Recurrence period of marked significant earthquakes in research region

Within subduction zones, there is an elevated likelihood of earthquakes exceeding a magnitude of 8. Subduction zones are known for hosting substantial seismic events. The motion of subducting tectonic plates generates considerable energy, which, rather than being promptly discharged as seismic activity, can accumulate over time due to asperities. These asperities are in the lower crustal region [24].

4. Conclusion

This study analyzed the spatial and temporal variations of b-values and a-values along the west coast of northern Sumatra from 1964 to 2023 to evaluate seismicity and stress accumulation patterns. The results indicate that areas such as Nagan Raya and Aceh Singkil exhibit low b- and a-

values, implying high stress build-up and low earthquake frequency—conditions that may increase the likelihood of future significant events. Temporal analysis shows a general decline in *b*-values prior to major earthquakes, supporting their potential use as seismic precursors. These findings highlight the need for enhanced seismic hazard assessment in high-risk zones. Future studies should explore the integration of high-resolution mapping and machine learning techniques to better detect precursory patterns and strengthen early warning systems.

Acknowledgments

We sincerely thank USGS for providing the earthquake data used in this research. We also express our deep appreciation to Weimer & Wyss for their use of the ZMAP6.0 software and to Wessel & Smith for using the GMT program.

References

- [1] M. Madlazim, "Kajian awal tentang b value gempa bumi di Sumatra," *Jurnal Penelitian Fisika dan Aplikasinya (JPFA)*, vol. 3, no. 1, pp. 41–46, 2013.
- [2] K. Sieh and D. Natawidjaja, "Neotectonics of the Sumatran fault, Indonesia," *J Geophys Res Solid Earth*, vol. 105, no. B12, pp. 28295–28326, 2000.
- [3] N. A. Radziminovich, A. I. Miroshnichenko, and F. L. Zuev, "Magnitude of completeness, b-value, and spatial correlation dimension of earthquakes in the South Baikal Basin, Baikal Rift System," *Tectonophysics*, vol. 759, pp. 44–57, 2019.
- [4] U. Chasanah and E. Handoyo, "Analisis Tingkat Kegempaan Wilayah Jawa Timur berbasis Distribusi Spasial dan Temporal Magnitude Of Completeness (Mc), A-Value Dan B-Value," *Indonesian Journal of Applied Physics*, vol. 11, no. 2, pp. 210–222, 2021.
- [5] K. Z. Nanjo and A. Yoshida, "A b map implying the first eastern rupture of the Nankai Trough earthquakes," *Nat Commun*, vol. 9, no. 1, p. 1117, 2018.
- [6] H. Risanti and T. Prastowo, "Estimasi parameter a-value dan b-value untuk analisis studi seismisitas dan potensi bahaya bencana gempa tektonik di wilayah maluku utara," *Inovasi Fisika Indonesia*, vol. 10, no. 1, pp. 1–10, 2021.
- [7] J. M. Borgohain, K. Borah, R. Biswas, and D. K. Bora, "Seismic b-value anomalies prior to the 3rd January 2016, Mw= 6.7 Manipur earthquake of northeast India," *J Asian Earth Sci*, vol. 154, pp. 42–48, 2018.
- [8] K. Aki, "Maximum likelihood estimate of b in the formula log N= a-bM and its confidence limits," *Bull. Earthquake Res. Inst., Tokyo Univ.*, vol. 43, pp. 237–239, 1965.
- [9] S. Wiemer, "A software package to analyze seismicity: ZMAP," Seismological Research Letters, vol. 72, no. 3, pp. 373–382, 2001.
- [10] H. E. A. Hafiez and M. Toni, "Magnitude of completeness for the Northern stations of the Egyptian National Seismological Network," *Arabian Journal of Geosciences*, vol. 13, pp. 1–9, 2020.

- [11] D. Pennucci, L. R. Abreu, and P. Bazzurro, "A COMPARISON OF ITALIAN SEISMICITY RATES BASED ON SMOOTHED AND AREA SOURCE MODELLING METHODOLOGIES."
- [12] N. Hu, P. Han, R. Wang, F. Shi, L. Chen, and H. Li, "Spatial Heterogeneity of b Values in Northeastern Tibetan Plateau and Its Interpretation," *Entropy*, vol. 26, no. 3, Mar. 2024, doi: 10.3390/e26030182.
- [13] D. Ahmad Suriamihardja, A. Maulana, and A. Jaya, "Study of Correlation between Rock Type and b-Value on Seismic Characteristics of Matano Fault," *International Journal of Earth Sciences and Engineering*, vol. 11, no. 02, pp. 153–158, 2018, doi: 10.21276/ijee.2018.11.0209.
- [14] H. Hussain, Z. Shuangxi, M. Usman, and M. Abid, "Spatial variation of b-values and their relationship with the fault blocks in the western part of the tibetan plateau and its surrounding areas," *Entropy*, vol. 22, no. 9, Sep. 2020, doi: 10.3390/e22091016.
- [15] Z. Gui, Y. Bai, Z. Wang, and T. Li, "Seismic b-value anomalies in the Sumatran region: Seismotectonic implications," *J Asian Earth Sci*, vol. 173, pp. 29–41, 2019.
- [16] Z. H. El-Isa and D. W. Eaton, "Spatiotemporal variations in the b-value of earthquake magnitude–frequency distributions: Classification and causes," *Tectonophysics*, vol. 615, pp. 1–11, 2014.
- [17] Y. Bayrak, A. Yılmaztürk, and S. Öztürk, "Lateral variations of the modal (a/b) values for the different regions of the world," *J Geodyn*, vol. 34, no. 5, pp. 653–666, 2002.
- [18] S. Pailoplee and M. Choowong, "Earthquake frequency-magnitude distribution and fractal dimension in mainland Southeast Asia," *Earth, Planets and space*, vol. 66, pp. 1–10, 2014.
- [19] S. C. Jaumé and L. R. Sykes, "Evolving towards a critical point: A review of accelerating seismic moment/energy release prior to large and great earthquakes," *Seismicity patterns, their statistical significance and physical meaning*, pp. 279–305, 1999.
- [20] S. Ruiz-Barajas, N. Sharma, V. Convertito, A. Zollo, and B. Benito, "Temporal evolution of a seismic sequence induced by a gas injection in the Eastern coast of Spain," *Sci Rep*, vol. 7, no. 1, p. 2901, 2017.
- [21] M. Arroyo-Solórzano and L. Linkimer, "Spatial variability of the b-value and seismic potential in Costa Rica," *Tectonophysics*, vol. 814, p. 228951, 2021.
- [22] D. Schorlemmer, S. Wiemer, and M. Wyss, "Variations in earthquake-size distribution across different stress regimes," *Nature*, vol. 437, no. 7058, pp. 539–542, 2005.
- [23] L. Gulia and S. Wiemer, "The influence of tectonic regimes on the earthquake size distribution: A case study for Italy," *Geophys Res Lett*, vol. 37, no. 10, 2010.
- [24] S. Ozturk, "Statistical correlation between b-value and fractal dimension regarding Turkish epicentre distribution," *Earth Sciences Research Journal*, vol. 16, no. 2, pp. 103–108, 2012.
- [25] A. Arimuko, "Seismotektonik Bagian Barat Sumatra ditinjau dari Nilai-b dan Nilai-a yang didapatkan melalui Inversi Matriks dan Regresi Linier," *DIFFRACTION: Journal for Physics Education and Applied Physics*, vol. 4, no. 2, pp. 42–51, 2022.

- [26] A. V. Simangunsong, R. Priadi, A. A. I. Dwilyantari, and A. Marsono, "Determination of temporal value of a-value and b-value to identify the level brittle of rock and seismic activity in the Palu region," *J. Phys.: Theor. Appl*, vol. 3, no. 1, pp. 1–8, 2019.
- [27] T. Utsu, "Analyses of the distribution of earthquakes in magnitude, time, and space with special consideration to clustering characteristics of earthquake occurrence," *J. Faculty of Science, Hokkaido Univ. Ser. VII (Geophysics)*, vol. 3, no. 5, pp. 379–441, 1971.
- [28] J. Chen and S. Zhu, "Spatial and temporal b-value precursors preceding the 2008 Wenchuan, China, earthquake (Mw= 7.9): implications for earthquake prediction," *Geomatics, Natural Hazards and Risk*, vol. 11, no. 1, pp. 1196–1211, 2020.
- [29] H. Huang, R. Burgmann, L. Meng, B. Rousset, and K. Wang, "Spatio-temporal foreshock evolution of the 2019 M 6.4 and M 7.1 Ridgecrest, California earthquakes," in *AGU Fall Meeting Abstracts*, 2019, pp. S43C-08.
- [30] R. Ormeni, S. Öztürk, A. Fundo, and K. Celik, "Spatial and temporal analysis of recent seismicity in different parts of the Vlora-Lushnja-Elbasani-Dibra Transversal Fault Zone, Albania," *Austrian Journal of Earth Sciences*, 2017.